

## Vibronic coupling in the ground and excited states of the naphthalene cation

Demetrio A. da Silva Filho,<sup>a</sup> Rainer Friedlein,<sup>b</sup> Veaceslav Coropceanu,<sup>\*a</sup> Gunnar Öhrwall,<sup>c</sup> Wojciech Osikowicz,<sup>b</sup> Christian Suess,<sup>b</sup> Stacey L. Sorensen,<sup>d</sup> Svante Svensson,<sup>c</sup> William R. Salaneck<sup>b</sup> and Jean-Luc Brédas<sup>\*a</sup>

<sup>a</sup> School of Chemistry and Biochemistry, Georgia Institute of Technology, Atlanta, Georgia 30332-0400.

E-mail: veaceslav.coropceanu@chemistry.gatech.edu; jean-luc.bredas@chemistry.gatech.edu

<sup>b</sup> Department of Physics (IFM), Linköping University, S-581 83 Linköping, Sweden

<sup>c</sup> Department of Physics, Uppsala University, Box 530, S-751 21 Uppsala, Sweden

<sup>d</sup> Department of Synchrotron Radiation Research, Institute of Physics, Lund University, Box 118, S-221 00 Lund, Sweden

Received (in Cambridge, UK) 15th March 2004, Accepted 30th April 2004

First published as an Advance Article on the web 24th June 2004

The hole–vibrational coupling in naphthalene is studied using high-resolution gas-phase photoelectron spectroscopy and density functional theory calculations (DFT), and a remarkable increase of the coupling with low-frequency vibrations is observed in the excited states.

Oligoacenes are currently of great interest due to their potential application in organic electronic devices such as field-effect transistors.<sup>1</sup> Since in  $\pi$ -conjugated systems any charge injection or electronic excitation process leads to marked geometry relaxations,<sup>2</sup> the efficiency of charge or energy transport and ultimately the performance of electronic devices are controlled to a large extent by electron (hole)–vibration interactions. Vibronic coupling in oligoacenes has been addressed in several studies;<sup>3–6</sup> however, a complete understanding is still lacking, especially when considering the excited states.

In a recent work,<sup>6</sup> we investigated the relaxation processes in the radical-cation ground state upon positive ionization of anthracene, tetracene, and pentacene; these were studied using an approach that combines high-resolution gas-phase photoelectron spectroscopy measurements with first-principles quantum-mechanical calculations. In this Communication, we extend this approach to the smallest member of the acene family, naphthalene (inset of Fig. 1), and to excited states. We report here on the hole–vibration coupling in the ground and lowest excited states of the radical-cation.

The gas-phase photoelectron valence band spectrum was obtained using  $h\nu = 60$  eV-photons from the MAX-II storage ring at MAX-Lab in Lund, Sweden. The Scienta SES-200 photoelectron spectrometer of beamline I411 was tuned to the magic angle between the electric field vector of the light and the direction of the photoelectron emission. An overall resolution of about 26 meV was employed. A gas cell with an external feed was used allowing high gas densities (local pressure  $> 1 \times 10^{-5}$  mbar) and moderate temperatures of  $40 \pm 20$  °C in the target zone.

The gas-phase photoelectron spectrum of naphthalene is shown in Figs. 1 and 2. The spectrum is, in general, similar to those that

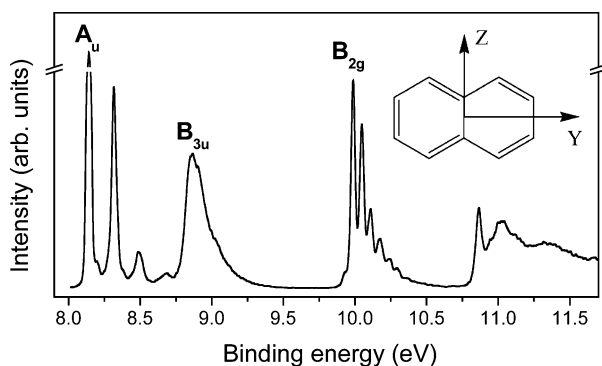


Fig. 1 Gas-phase photoelectron emission spectrum of naphthalene.

have been previously reported,<sup>7</sup> although the individual peaks in the vibrational fine structure are better resolved. As in the case of longer oligoacenes,<sup>6</sup> the first ionization band of naphthalene exhibits a high frequency progression of about  $1500 \text{ cm}^{-1}$  (180 meV), which lies in the region expected for C–C stretching modes. However, in contrast to anthracene, tetracene, and pentacene, a contribution from a second vibration at about  $500 \text{ cm}^{-1}$  (60 meV) is also clearly resolved in naphthalene. In addition, as seen from the profile of the third ionization, the interaction with this mode completely dominates the geometrical relaxation of the  ${}^2B_{2g}$  state upon ionization. Thus, coupling of the hole with this mode is even larger in the excited states. Interestingly, in striking contrast with the first and third ionization bands the second ionization band is rather structureless.

The geometry optimizations and normal-mode analysis of the neutral and radical-cation naphthalene states were performed with the Gaussian-98 program<sup>8</sup> at the DFT-B3LYP level using a 6-31G\*\* basis set. The relaxation energies of the radical-cation states and their partition into the contributions from each vibrational mode were derived in two ways. The first approach (model 1) exploits the adiabatic potential energy surfaces of both the neutral and cation states. The second approach (model 2) is based on the concept of orbital vibronic constants.<sup>9,10</sup> The results of the DFT/B3LYP calculations of the relaxation energies in naphthalene are reported in Fig. 3. The results obtained from both models are in excellent mutual agreement. The normal mode calculations reveal that the main contribution to the relaxation energy  $\lambda$  of the cation

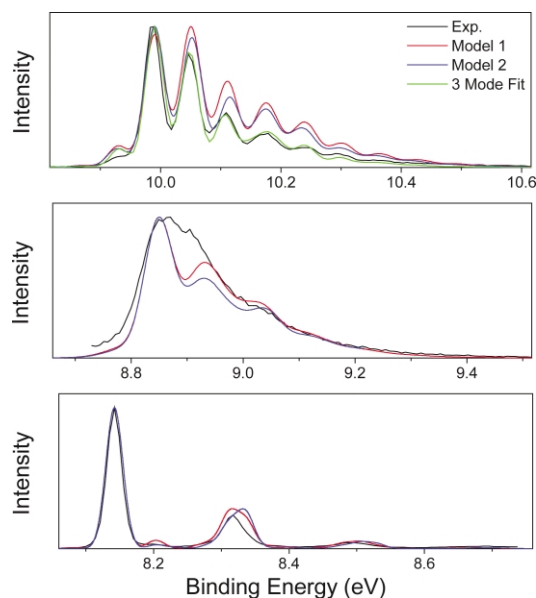
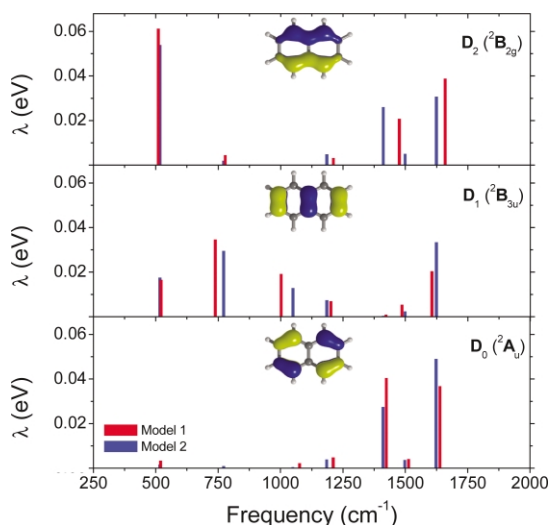


Fig. 2 Experimental and theoretical spectral profiles of the first three ionizations of naphthalene (see text for notations).



**Fig. 3** Individual contributions of the totally symmetric modes to the relaxation energy, from DFT-B3LYP calculations.

$^2A_u$  ground state comes from two high-frequency modes of  $1420\text{ cm}^{-1}$  and  $1640\text{ cm}^{-1}$ . The total relaxation energy of 91 meV (model 1)<sup>11</sup> of this state follows the trend predicted<sup>12</sup> and observed<sup>6a</sup> in longer oligoacenes (anthracene, 70 meV; tetracene, 56 meV; pentacene, 49 meV). The relaxation energy steadily increases to 103 meV and 128 meV for the excited  $^2B_{3u}$  and  $^2B_{2g}$  states, respectively. The calculations also reveal a significant redistribution of the excited-state relaxation energy towards lower-frequency vibrations. In agreement with the experimental observations, the lowest-energy totally symmetric mode of  $500\text{ cm}^{-1}$  is predicted to be active in all three states. As seen from Fig. 2, the vibronic constant of this mode significantly increases on going from the ground to the second excited radical-cation state. However, it seems that the DFT calculations overestimate to some extent the vibronic coupling with this mode; the DFT values for the Huang–Rhys factor of  $S = 0.97$  (model 1) and  $S = 0.83$  (model 2) in the  $^2B_{2g}$  state are larger than the value of  $S = 0.73$  derived from the best fit of the band to a (three-mode) harmonic model (see Fig. 2).

We have also carried out the Frank–Condon simulation of the shape of the first three ionizations using the frequencies and Huang–Rhys factors derived from the DFT calculations (for both models). For the first and third ionizations, the positions and shapes of the individual peaks are well reproduced. However, there is a marked discrepancy between the experimental and theoretical spectra in the case of the second ionization. The failure of the adiabatic model and the lack of vibrational fine structure in the spectral band are characteristic signatures of non-adiabatic interactions.<sup>13</sup> Indeed, in agreement with previous studies,<sup>4a</sup> we have found a considerable vibronic interaction between the  $^2A_u$  and  $^2B_{3u}$  states via pseudo Jahn–Teller  $b_{3g}$  modes, the most active of which being the vibration at  $1520\text{ cm}^{-1}$ . Moreover, our calculations show that the adiabatic potential surfaces of the  $^2A_u$  and  $^2B_{3u}$  states exhibit a conical intersection only a few meV above the minimum of the upper state. As a consequence, non-adiabatic interactions strongly affect the density of the vibrational manifold of the  $^2B_{3u}$  state which explains the broadening of the  $^2B_{3u}$  spectral band. Although the minimum of the  $^2A_u$  ground state is well separated from the conical intersection by 0.74 eV, the non-adiabatic effects should also slightly perturb its vibrational levels calculated in the adiabatic approximation. Thus, the lack of resolved splitting between the high-frequency modes at  $1420\text{ cm}^{-1}$  and  $1640\text{ cm}^{-1}$  in

the experimental spectrum, is most likely due to non-adiabatic interactions as well.

The work at Georgia Tech is partly supported by the National Science Foundation, through the STC for Materials and Devices for Information Technology – DMR-0120967, the MRSEC at the University of Minnesota – DMR-0212302, and grant CHE-0343321, and the IBM Shared University Research program. The experimental work is performed in collaboration with the Center for Advanced Molecular Materials (CAMM) funded by SSF; financial support from the Swedish Science Research Council (VR) is acknowledged. The authors also thank M. Tchapyguine (Uppsala University, Sweden) for technical assistance.

## Notes and references

- (a) H. Klauk, D. J. Gundlach and T. N. Jackson, *IEEE Electron. Device Lett.*, 1999, **0**, 289; (b) H. Klauk, D. J. Gundlach, M. Bonse, C. C. Kuo and T. N. Jackson, *Appl. Phys. Lett.*, 2000, **6**, 1692.
- (a) W. P. Su, J. R. Schrieffer and A. J. Heeger, *Phys. Rev. Lett.*, 1979, **2**, 1698; (b) W. R. Salaneck, R. H. Friend and J. L. Brédas, *Phys. Rep.*, 1999, **9**, 231.
- (a) L. Andrews and T. A. Blankenship, *J. Am. Chem. Soc.*, 1981, **3**, 5977; (b) S. M. Beck, D. E. Powers, J. B. Hopkins and R. E. Smalley, *J. Chem. Phys.*, 1980, **3**, 2019; (c) M. Stockburger, H. Gattermann and W. Klusmann, *J. Chem. Phys.*, 1975, **3**, 4519; (d) F. Salama and L. J. Allamandola, *J. Chem. Phys.*, 1991, **4**, 6964; (e) M. C. R. Cockett, H. Ozeki, K. Okuyama and K. Kimura, *J. Chem. Phys.*, 1993, **8**, 7763.
- (a) F. Negri and M. Z. Zgierski, *J. Chem. Phys.*, 1994, **0**, 1387; (b) F. Negri and M. Z. Zgierski, *J. Chem. Phys.*, 1996, **4**, 3486; (c) F. Negri and M. Z. Zgierski, *J. Chem. Phys.*, 1997, **7**, 4827; (d) M. Z. Zgierski, *J. Chem. Phys.*, 1997, **7**, 7685.
- (a) T. Kato and T. Yamabe, *J. Chem. Phys.*, 2001, **5**, 8592; (b) T. Kato and T. Yamabe, *J. Chem. Phys.*, 2003, **8**, 3804; (c) T. Kato and T. Yamabe, *J. Chem. Phys.*, 2003, **9**, 11318.
- (a) V. Coropceanu, M. Malagoli, D. A. da Silva Filho, N. E. Gruhn, T. G. Bill and J. L. Brédas, *Phys. Rev. Lett.*, 2002, **9**, 275503/1; (b) N. E. Gruhn, D. A. da Silva Filho, T. G. Bill, M. Malagoli, V. Coropceanu, A. Kahn and J. L. Brédas, *J. Am. Chem. Soc.*, 2002, **4**, 7918; (c) M. Malagoli, V. Coropceanu, D. A. da Silva Filho and J. L. Brédas, *J. Chem. Phys.*, 2004, 7490.
- (a) T. Bally, C. Carra, M. P. Fülischer and Z. Zhu, *J. Chem. Soc., Perkin Trans. 2*, 1998, 1759; (b) C. R. Brundle, M. B. Robin and N. A. Kuebler, *J. Am. Chem. Soc.*, 1972, **4**, 1466; (c) F. Brogli, E. Heilbronner and T. Kobayashi, *Helv. Chim. Acta*, 1972, **5**, 274; (d) R. Boschi, J. N. Murrell and W. Schmidt, *Discuss. Faraday Soc.*, 1972, **4**, 116.
- M. J. Frisch, G. W. Trucks, H. B. Schlegel, G. E. Scuseria, M. A. Robb, J. R. Cheeseman, V. G. Zakrzewski, J. A. Montgomery, Jr., R. E. Stratmann, J. C. Burant, S. Dapprich, J. M. Millam, A. D. Daniels, K. N. Kudin, M. C. Strain, O. Farkas, J. Tomasi, V. Barone, M. Cossi, R. Cammi, B. Mennucci, C. Pomelli, C. Adamo, S. Clifford, J. Ochterski, G. A. Petersson, P. Y. Ayala, Q. Cui, K. Morokuma, P. Salvador, J. J. Dannenberg, D. K. Malick, A. D. Rabuck, K. Raghavachari, J. B. Foresman, J. Cioslowski, J. V. Ortiz, A. G. Baboul, B. B. Stefanov, G. Liu, A. Liashenko, P. Piskorz, I. Komaromi, R. Gomperts, R. L. Martin, D. J. Fox, T. Keith, M. A. Al-Laham, C. Y. Peng, A. Nanayakkara, M. Challacombe, P. M. W. Gill, B. Johnson, W. Chen, M. W. Wong, J. L. Andres, C. Gonzalez, M. Head-Gordon, E. S. Replogle and J. A. Pople, *Gaussian 98, Revision A.11*; Gaussian, Inc.; Pittsburgh PA, 2001.
- I. B. Bersuker, *The Jahn–Teller Effect and Vibronic Interactions in Modern Chemistry*, Plenum Press, New York, 1984.
- The first model is generally more accurate since it is based on vibrational mode calculations for each cation state, while the second model makes use of only the normal modes of the neutral molecule. Examples of the application of model 1 and model 2 to oligoacenes can be found in ref. 6 and ref. 5, respectively.
- The relaxation energies obtained in the framework of model 2 are 87 meV, 105 meV, and 122 meV for the  $^2A_u$ ,  $^2B_{3u}$ , and  $^2B_{2g}$  states, respectively.
- A. Devos and M. Lannoo, *Phys. Rev. B*, 1988, **8**, 8236.
- H. Köppel, W. Domcke and L. S. Cederbaum, *Adv. Chem. Phys.*, 1984, **7**, 59.